Available online at www.eccomasproceedia.org
Eccomas Proceedia COMPDYN (2023) 3908-3915

ECCOMAS
Proceedia

COMPDYN 2023
9th ECCOMAS Thematic Conference on
Computational Methods in Structural Dynamics and Earthquake Engineering
M. Papadrakakis, M. Fragiadakis (eds.)
Athens, Greece, 12-14 June 2023

INVESTIGATION OF FAILURE OCCURRENCE MECHANISM OF HISTORIC MASONRY BUILDINGS AND PERFORMANCE OF REINFORCEMENT MEASURES USING DEM

J. Kiyono[1] and A. Furukawa[2]

[1] Department of Urban Management, Kyoto University
Kyotodaigaku-katsura, Nishikyo-ku, Kyoto 615-8540, JAPAN
e-mail: kiyono.junji.5x@kyoto-u.jp

[2] Department of Urban Management, Kyoto University
Kyotodaigaku-katsura, Nishikyo-ku, Kyoto 615-8540, JAPAN
e-mail: furukawa.aiko.3w@kyoto-u.ac.jp

Abstract

There are many historic masonry buildings worldwide. Some types of masonry buildings have particularly low earthquake resistance. Such structures collapse even at low-ground motion intensities and rapidly at high intensities. Therefore, improving the earthquake resistance of these primarily weak masonry buildings is necessary to prevent their damage and leave them for posterity. However, knowledge is still limited on how the failure begins and proceeds, how buildings collapse, and how earthquake resistance can be improved effectively. With this background, this study aims to investigate the seismic behaviors of masonry buildings and compare the effectiveness of reinforcement measures by numerical simulations.

Keywords: Masonry building, Failure behavior, Reinforcing measures, Distinct element method, Earthquake.

ISSN:2623-3347
Peer-review under responsibility of the organizing committee of COMPDYN 2023.
doi: 10.7712/120123.10689.20085

1 INTRODUCTION

There are many historic masonry buildings worldwide. Due to their low earthquake resistance [1], they get damaged even at low intensities of ground motion and collapse rapidly at high intensities [2][3][4]. Therefore, improving the earthquake resistance of these primarily weak masonry buildings is necessary to prevent their damage and leave them for posterity. However, knowledge is still limited on how the failure begins and proceeds, how buildings collapse, and how earthquake resistance can be improved effectively. With this background, this study aims to investigate the seismic performance of masonry buildings and compare the effectiveness of reinforcement measures by numerical simulations.

The finite element method (FEM) is the most common numerical analysis method. It has been used for the analysis of masonry structures [5][6][7][8]. The FEM can deal with both elastic and plastic behaviors, but it has difficulty solving failure and collapse phenomena since it is based on the mechanics of the continuum. A method based on the mechanics of the dis-continuum is more suitable for analyzing failure and collapse phenomena. An example of a numerical method for a dis-continuum is the distinct element method (DEM) [9]. However, the DEM also has disadvantages. A way of determining the spring constant from the material properties has not been established in the DEM, and the values need to be quantified experimentally [10][11]. Therefore, the reliability of the results is not high.

As an alternative, the present paper uses a refined DEM [12][13], which simulates a series of seismic behaviors in three-dimension—from elastic to failure to collapse behaviors. This method still cannot handle Poisson's effect like the original DEM, but unlike the original DEM, the spring constant of each spring is theoretically determinable. Using the refined DEM, this paper simulates the seismic behavior of historical masonry buildings and compares the performances of reinforcement measures.

2 REFINED DEM

This study employs a refined DEM [12] to simulate a series of structural dynamic behaviors from elastic to failure to collapse phenomena. A structure is modeled as an assembly of rigid elements, and interaction between the elements is modeled with multiple springs and dashpots attached to the elements' surfaces. The elements are rigid, but the method allows the simulation of structural deformation by allowing penetration between elements.

Fig. 1 (a) shows a spring for computing the restoring force (restoring spring), which models the elasticity of elements. The restoring spring is set between continuous elements. Structural failure is modeled as the breakage of the restoring spring, at which time the restoring spring is replaced with a contact spring and a contact dashpot (Fig. 1 (b)). Fig. 1 (b) shows the spring and dashpot for computing the contact force (contact spring and dashpot) and modeling the contact, separation and recontact between elements. The dashpots are introduced to express energy dissipation due to the contact. Structural collapse behavior is obtained using these springs and dashpots. The elements shown in Figs. 1 (a) and (b) are rectangular parallelepipeds, but the method does not limit the geometry of the elements.

The surface of an element is divided into small segments, as shown in Fig. 1 (c). The segment in the figure is rectangular, but the method does not limit the geometry of the segment. The black points indicate the representative point of each segment, and the relative displacement or contact displacement between elements is computed for these points. Such points are referred to as contact points or master points in this study. One restoring spring and one combination of contact spring and dashpot are attached to one segment (Fig. 1 (d)) at each of the representative points in Fig. 1 (c). The spring constant for each segment is derived based on the stress-strain relationship of the material and the segment area.

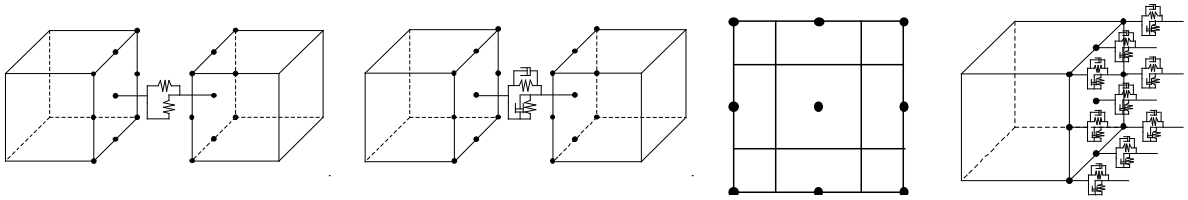

(a) Restoring spring (b) Contact spring and dashpot (c) Segments and contact points (d) Multiple springs and multiple dashpots

Figure 1: Basic concept of the analysis method [12]

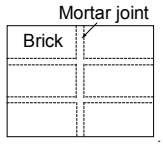

(a) Masonry structure

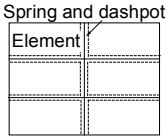

(b) Analytical model

Figure 2 Analytical modeling of masonry structures

Table 1 Material properties

Variable	Adobe brick	Mortar	Wood	FRP
Mass density (kg/m^3)	1.8×10^3	1.8×10^3	7.0×10^2	1.8×10^3
Young's modulus (N/m^2)	9.8×10^7	9.8×10^7	6.3×10^8	2.5×10^{10}
Poisson's ratio	0.25	0.25	0.3	0.3

Table 2 Strength of mortar, wood, and FRP

Variable	Mortar	Wood	FRP
Tensile strength f_t (N/m^2)	4.6×10^3	1.1×10^7	1.27×10^5
Shear strength c (N/m^2)	2.9×10^3	9.0×10^6	3.04×10^4
Friction angle ϕ	32°	0°	32° used
Compressive strength (N/m^2)	4.9×10^5	4.5×10^7	4.9×10^5

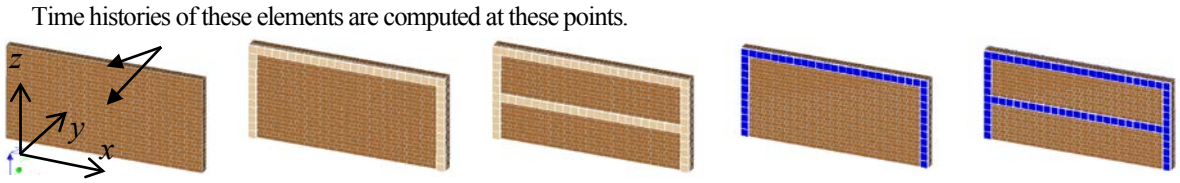

(a)Non-reinforced model (b)Reinforced model with timbers (T1) (c)Reinforced model with timbers (T2) (d) Reinforced model with FRP strips (F1, F3) (e) Reinforced model with FRP strips (F2, F4)

Figure 3 Analytical masonry wall models

The behavior of an element consists of translational and rotational behaviors. Each element's translational and rotational behaviors are computed explicitly by solving Newton's law of motion and Euler's equation of motion. Forces acting on each element are obtained by summing the restoring force, contact force, and other external forces, such as the gravitational force and the earthquake's inertial force.

3 ANALYSIS OF MASONRY WALL

3.1 Modeling Strategy of Masonry

In this study, individual components of the masonry structure shown in Fig. 2 (a) (i.e., brick and mortar joints) are modeled as shown in Fig. 2 (b). The bricks are modeled with rigid elements, and the mortar joint between elements is modeled with multiple springs and dashpots. The size of one element is the sum of the brick size and mortar thickness. The multiple springs and dashpots interact with the surfaces of adjacent elements. The elements are modeled with rigid rectangular parallelepipeds. Faces surrounding the elements are divided into segments. The size of the segments is set to 1/4 of the shortest edge length, according to a past study [12].

3.2 Analytical Masonry Wall Models

As shown in Fig. 3, one masonry wall model without reinforcement, 2 reinforcement models with timbers, and 4 reinforcement models with FRP strips were considered. The directions (x, y, z) are also shown in Fig. 3(a). Reinforcement using timbers is frequently used where timber materials are easily available at a reasonable price. The reinforcement using FRP strips is recently gathered much attention due to its high performance.

The non-reinforced model has a width of 5m, a height of 2.4m, and a thickness of 0.2m. The walls are mainly composed of bricks with dimensions of 0.2 m × 0.1 cm × 0.1 m. There are mortar joints with a thickness of 0.01 m between the bricks.

There are two reinforced models using timbers. Model T1 has two vertical columns and one horizontal beam on the top, and the reinforcement is one-sided. Model T2 has an additional horizontal beam in the middle height of the wall. Both columns and beams have 0.2m width and 0.1m thickness and are divided into many elements of 0.2m length to express the deformation and breakage. Therefore, the size of timber elements is 0.2 m × 0.1 cm × 0.1 m.

Four reinforced models use FRP strips. Model F1 is a one-sided reinforcement model with two vertical strips and one horizontal strip on the top. Model F2 is a model with an additional horizontal strip in the middle height of the wall. Model F3 has a reinforcement of F1 on both sides of the wall. Model F4 has a reinforcement of F2 on both sides of the wall. The FRP strips have 0.2m width and 0.02m thickness and are divided into many elements of 0.2m length to express the deformation and breakage. Therefore, the size of FRP elements is 0.2 m × 0.02 cm × 0.1 m.

3.3 Material Properties and Strength

Table 1 presents the material properties. The mass density and Young's modulus of adobe bricks are chosen based on experimental results for adobe bricks [14]. The mass density and Young's modulus of the mortar are assumed to be the same as those for the adobe bricks. The material properties of the timber and FRP elements are listed in Table 1.

Ghannand et al. [14] conducted a laboratory experiment to measure the strength of the adobe bricks used in rural regions in Iran. The results are shown in Table 2. Since the friction angle was not given, the value of a damaged adobe building during a reconnaissance survey of the Bam earthquake in Iran [3] is used.

General values shown in Table 2 are used for the timber and FRP elements.

3.4 Input Ground Motion

The Building and Housing Research Center in Iran recorded the main shock of the Bam earthquake [2]. The maximum accelerations of the two horizontal (T, L) and vertical (V) components of the earthquake after correction were 6.23 m/s^2 (T), 7.78 m/s^2 (L), and 9.80 m/s^2 (V) (Figs. 4 (a)–(c)). The direction of the accelerometer for the L component is N278E. The vertical component is very large. For the horizontal components, the peak ground acceleration of the L component is greater than that of the T component. The T, L, and V components are input in the x, y, and z directions.

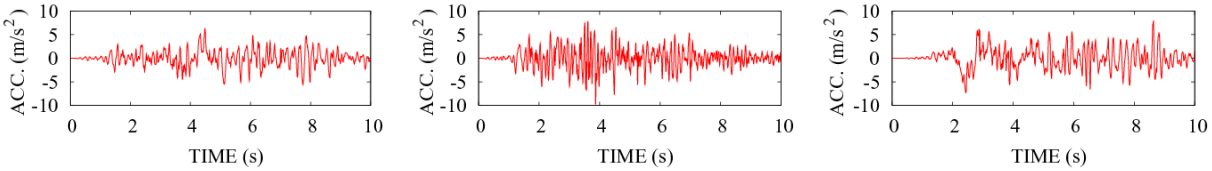

(a) T componentt (b) L component (c) V component

Figure 4 Time histories of input ground motion

3.5 Seismic Behavior of Masonry Wall Models

The seismic behavior is shown in Fig. 5. The non-reinforced model vibrated in the out-of-plane direction, a horizontal crack was generated at the middle height, and the wall fell.

Both reinforced models with timbers (T1, T2) successfully prevented the collapse, but diagonal cracks can be seen in the wall.

Two single-sided reinforced models with FRP strips (F1, F2) could not prevent the wall from falling. On the contrary, double-sided reinforced models with FRP strips (F3, F4) did not fall. This outcome does not mean that reinforcement from both sides is always necessary. In the case of the building, walls are connected with the adjacent walls, reducing the walls' out-of-plane deformation. In this case, the single-sided reinforcement is sufficient to prevent the wall from collapsing. T1 and T2 are also single-sided reinforced models, but the timbers are thicker than FRP strips, which may be why the T1 and T2 models did not fall. No clear difference can be seen between models T1 and T2, F1 and F2, and F3 and F4. This outcome indicates that one horizontal timber or FRP strip is sufficient for this model.

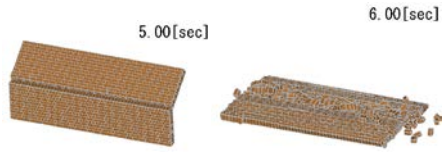

(a) Non-reinforced model (Front view)

(b)Reinforced model with timbers (T1)
(left: front view, right: rear view)

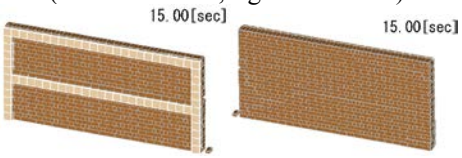

(c)Reinforced model with timbers (T2)
(left: front view, right: rear view)

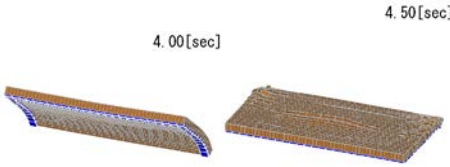

(d) Single-sided reinforced model with FRP strips (F1)

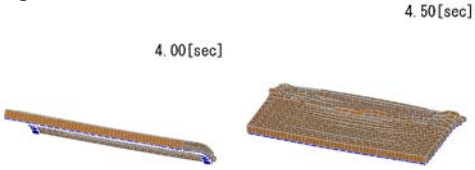

(e) Single-sided reinforced model with FRP strips (F2)

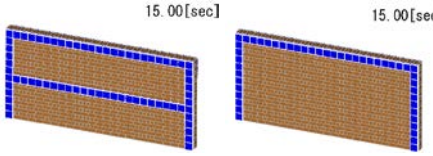

(f) Double-sided reinforced model with FRP strips (F3)
(g) Double-sided reinforced model with FRP strips (F4)

Figure 5 Seismic behavior of masonry wall models

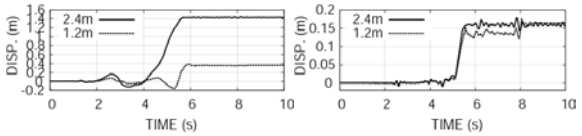

(a) Non-reinforced model

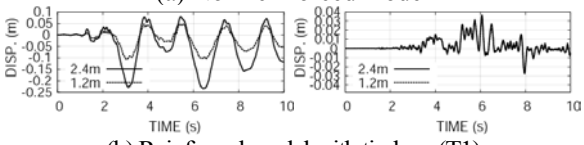

(b) Reinforced model with timbers (T1)

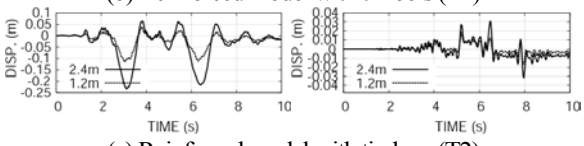

(c) Reinforced model with timbers (T2)

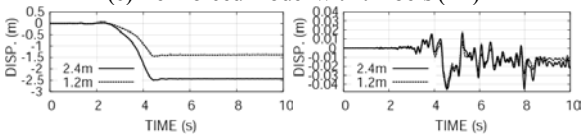

(d) Single-sided reinforced model with FRP strips (F1)

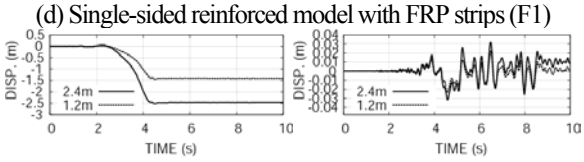

(e) Single-sided reinforced model with FRP strips (F2)

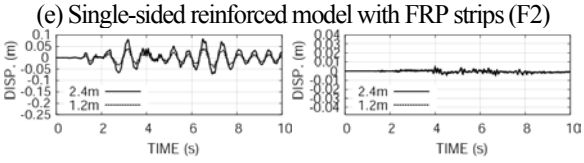

(f) Double-sided reinforced model with FRP strips (F3)

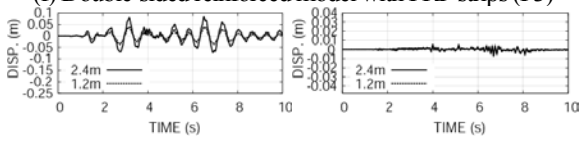

(g) Double-sided reinforced model with FRP strips (F4)

Figure 6 Displacement history of masonry walls
(left: x-direction, right: y-direction)

3.6 Displacement History of Masonry Wall Models

Next, displacement histories at two points (shown in Fig.3(a)) are compared. Fig. 6 shows the displacement history in the *x*- and *y*-direction. From the comparison among Figs. 6(a), (d), and (e), it is found that reinforced models F1 and F2 collapsed earlier than the non-reinforced model. The reason for this is considered as follows. The non-reinforced model moves in both directions during vibration. However, the single-sided reinforced models tend to move in a single direction and start tilting earlier than the non-reinforced model. The analyzed model is a single wall with thin FRP strips, which may be why the FRP strips could not prevent the wall from falling down. Even though the wall fell, the effect of FRP strips can be seen. At least, the single-sided FRP reinforcement could prevent the wall from scattering. The displacements of F3 and F4 are much smaller than those of T1 and T2 (Fig.6 (b)(c)(f)(g)). The FRP is stiffer and largely reduces the deformation than the timbers so that fewer cracks can be seen in F3 and F4 compared to T1 and T2. The models with one and two horizontal reinforcing elements showed almost the same displacement level.

4 ANALYSIS OF MASONRY BUILDINGS

4.1 Analytical Models

Fig. 7 illustrates the masonry building model with a flat roof made of wooden beams. The direction (*x*, *y*, *z*) is also shown in Fig. 7. The walls facing the *y* direction support the roof, so these walls are referred to as bearing walls, and the other two walls are referred to as nonbearing walls. The external width of the building is 5.4 m × 3.4 m. The internal width is 5.0 m × 3.0 m. The height of the walls is 2.4 m. The depth of the walls is 0.2 m. The walls are composed of bricks with dimensions of 0.2 m × 0.1 cm × 0.1 m. There are mortar joints with a thickness of 0.01 m between the bricks.

One bearing wall has a door and a window opening. The size of the door is 1.2 m (width) × 2.0 m (height). The size of the window is 1.0 m × 1.0 m and the height of the lower side of the window is 1.0 m. There are wooden beams above the openings that support the elements above the openings. The dimensions of the beams above the openings are 0.2 m × 0.1 m × 1.4 m (in length). These beams are divided into segments with a length of 0.2 m to express their deformation and separation. The roof consists of 27 beams that run in the *y* direction. The beams' dimensions are 0.2 m × 0.2 m × 3.4 m (in length). These roof beams are divided into segments with a length of 0.2 m to express their deformation and separation. The roof beams rest on the walls, and there are mortar joints between the beams and walls.
In this section, the *L*, *T,* and *V* components are input in the *x*, *y,* and *z* directions.

4.2 Seismic Behavior of Non-Reinforced Model

The seismic behavior is shown in Fig. 8. The elements with a red area mean that the tensile failure occurred in this area. Only tensile failure occurred, and neither shear nor compressive failure could be seen. The diagonal cracks can be seen around the wall and door openings. The structure collapsed in the *y*-direction due to the out-of-plane deformation of the bearing walls. The seismic behavior is summarized as follows. Diagonal and horizontal cracks in the bearing wall with openings are generated at 2.0 s. Vertical cracks in the bearing wall were generated before 3.6 s. The bearing wall then deformed in the out-of-plane direction at 6.0 s and fell in this direction. The roof collapsed with the failure of the bearing wall with the openings.

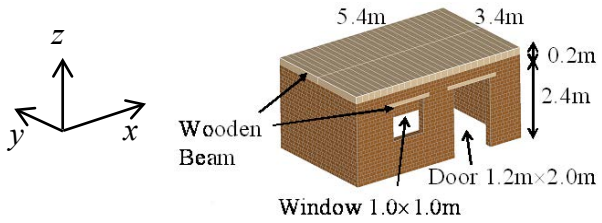

Figure 7 Analytical masonry building models

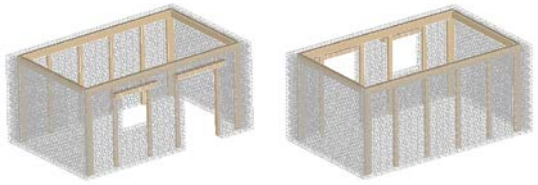

(a) front view (b) rear view

Figure 9 Analytical model of reinforced building

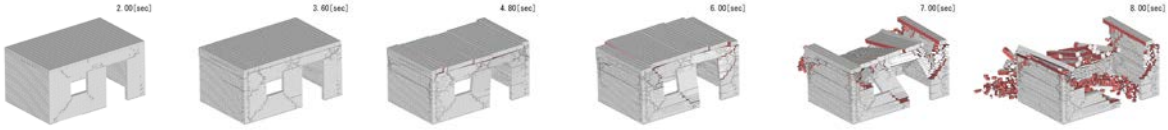

Figure 8 Seismic behavior of non-reinforced building

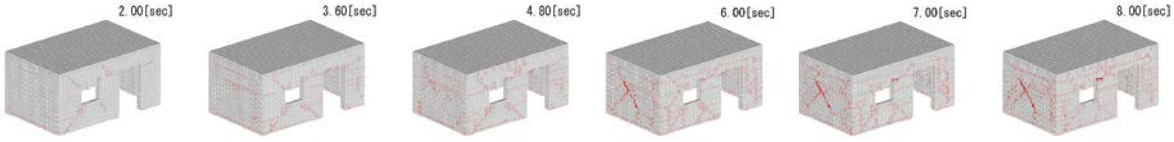

Figure 10 Seismic behavior of reinforced building with timbers

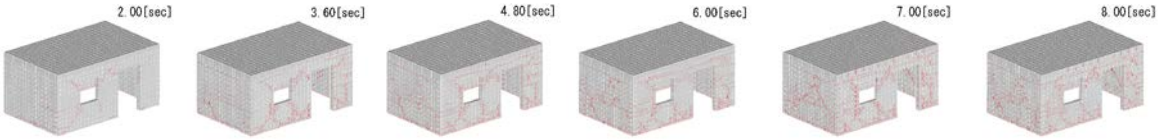

Figure 11 Seismic behavior of reinforced building with FRP strips

4.3 Reinforced Models

Two reinforced models with timbers and FRP strips are considered, as shown in Fig.9. Each bearing wall is reinforced with 6 vertical and 1 horizontal timbers or FRP strips. The vertical columns in the edge and horizontal beams have a width of 0.2m. The other columns have a width of 0.1m. The thickness of all timber columns and beams is 0.1m. The FRP strips have the same width as the timbers but have a thickness of 0.02m. Reinforcement was done inside the structure not to ruin the value of a historic structure.

4.4 Seismic Behavior of Reinforced Models

The seismic behaviors of the reinforced models are shown in Figs. 10 and 11. Both reinforced models did not collapse. The tensile failure occurred in both models, but the reinforced model with timbers has clearer diagonal cracks in the walls than the reinforced model with FRP strips since the FRP has a larger stiffness.

5 CONCLUSIONS

The seismic behavior of masonry walls and building models are analyzed, and the effectiveness of the reinforcement measures using timbers and FRP strips are compared. Since the FRP strips have larger stiffness than the timbers, FRP strips reduced the structural deformation and the number of cracks more effectively than the timbers.

REFERENCES

[1] R.R. Parajuli, A. Furukawa, D. Gautam, Experimental characterization of monumental brick masonry in Nepal. *Structures*, **28**, 1314-1321, 2020. https://doi.org/10.1016/j.istruc.2020.09.065

[2] BHRC, The very urgent preliminary report on Bam earthquake of Dec 26, 2003, 2003. http://www.bhrc.gov.ir.

[3] J. Kiyono, A. Kalantari, Collapse mechanism of adobe and masonry structures during the 2003 Iran Bam earthquake. *Bulletin of Earthquake Research Institute, University of Tokyo*, **79**, 157-161, 2004.

[4] A. Furukawa, J. Kiyono, R.R. Parajuli, H.R. Parajuli, K. Toki, Evaluation of damage to a historic masonry building in Nepal through comparison of dynamic characteristics before and after the 2015 Gorkha Earthquake. *Frontiers in Built Environment*, **3:62**, 2017. doi:10.3389/fbuil.2017.00062.

[5] P.B. Lourenco, Analysis of masonry structures with interface elements, theory and applications. The Delft University of Technology, Faculty of Civil Engineering, TU-DELFT report no.03-21-22-0-01, 1994.

[6] H.R. Parajuli, J. Kiyono, H. Taniguchi, K. Toki, A. Furukawa, P.N. Maskey, Parametric study and dynamic analysis of a historical masonry building of Kathmandu. *Journal of Disaster Mitigation of Cultural Heritage and Historic Cities*, **4**, 149-156, 2010.

[7] H.R. Parajuli, J. Kiyono, M. Tatsumi, Y. Suzuki, H. Umemura, H. Taniguchi, K. Toki, A. Furukawa, P.N. Maskey, Dynamic characteristic investigation of a historical masonry building and surrounding ground in Kathmandu. *Journal of Disaster Research*, **6(1)**, Dr6-1-4522, 2011. doi: 10.20965/jdr.2011.p0026

[8] A. Furukawa, J.J. Prasetyo, J. Kiyono, Performance of interlocking brick walls against out-of-plane excitation. *International Journal of GEOMATE*, **22(89)**, 100-105, 2022. https://doi.org/10.21660/2022.89.gxi413

[9] P.A. Cundall, O.D.L Strack, A discrete numerical model for granular assemblies. *Geotechnique*, **29**, 47-65, 1979.

[10] A. Furukawa, Y. Ohta, Failure process of masonry buildings during earthquake and associated casualty risk evaluation. *Natural Hazards*, 49(1), 25-51, 2009. http://dx.doi.org/10.1007/s11069-008-9275-x

[11] A. Furukawa, R. Spence, Y. Ohta, E. So, Analytical study on vulnerability functions for casualty estimation in the collapse of adobe buildings induced by earthquake, *Bulletin of Earthquake Engineering*, **8(2)**, 451-479, 2010. http://dx.doi.org/10.1007/s10518-009-9156-z

[12] A. Furukawa, J. Kiyono, K. Toki K, Proposal of a numerical simulation method for elastic, failure and collapse behaviors of structures and its application to masonry walls. *Journal of Disaster Research*, **6(1)**, Dr6-1-4524, 2011. doi: 10.20965/jdr.2011.p0051

[13] A. Furukawa, J. Kiyono, K. Toki, Numerical simulation of the failure propagation of masonry buildings during an earthquake, *Journal of Natural Disaster Science*, **33(1)**, 11-36, 2012, http://dx.doi.org/10.2328/jnds.33.11

[14] M.A. Ghannad, A. Bakhshi, E.S.E. Mousavi, A. Khosravifar, Y. Bozorgnia, B.A.A. Taheri, A study on seismic vulnerability of rural houses in Iran. *Proceedings of the 1st European Conference on Earthquake Engineering and Seismology*, No. 680, 2006.